

Petrology and mineral chemistry of peraluminous Marziyan granites, Sanandaj-Sirjan metamorphic belt (NW Iran)

ESMAIEL DARVISHI¹✉, MAHMOUD KHALILI², ROY BEAVERS³ and MOHAMMAD SAYARI²

¹Department of Geology, Islamic Azad University, Aligoodarz branch, Aligoodarz, Iran; ✉geo.edarvishi@gmail.com

²Department of Geology, University of Isfahan, Isfahan, Iran; mahmoudkhalili@yahoo.com; m.sayari@gmail.com

³Department of Geological Sciences, Southern Methodist University, Dallas, USA; rbeavers@smu.edu

(Manuscript received November 7, 2014; accepted in revised form June 23, 2015)

Abstract: The Marziyan granites are located in the north of Azna and crop out in the Sanandaj-Sirjan metamorphic belt. These rocks contain minerals such as quartz, K-feldspars, plagioclase, biotite, muscovite, garnet, tourmaline and minor sillimanite. The mineral chemistry of biotite indicates Fe-rich (siderophyllite), low TiO_2 , high Al_2O_3 , and low MgO nature, suggesting considerable Al concentration in the source magma. These biotites crystallized from peraluminous S-type granite magma belonging to the ilmenite series. The white mica is rich in alumina and has muscovite composition. The peraluminous nature of these rocks is manifested by their remarkably high SiO_2 , Al_2O_3 and high molar A/CNK (> 1.1) ratio. The latter feature is reflected by the presence of garnet and muscovite. All field observations, petrography, mineral chemistry and petrology evidence indicate a peraluminous, S-type nature of the Marziyan granitic rocks that formed by partial melting of metapelitic rocks in the mid to upper crust possibly under vapour-absent conditions. These rocks display geochemical characteristics that span the medium to high-K and calc-alkaline nature and profound chemical features typical of syn-collisional magmatism during collision of the Afro-Arabian continental plate and the Central Iranian microplate.

Key words: Marziyan S-type granites, peraluminous mineral chemistry, partial crustal melting.

Introduction

Significant volumes of magma-derived rocks in the continental crust are represented by granite. Many different types of granite have been recognized based on their bulk compositions, their mineral assemblages, and the tectonomagmatic settings in which they occur (Chappell & White 1984; Barbarin 1999; Patiño Douce 1999 and others). One of these granite types is the peraluminous (corundum-normative) leucocratic granites-granodiorites (leucogranites) which are characterized by primary muscovite and biotite, with minor garnet, rare cordierite, and very rare andalusite, all of which have been used as significant indicators of pressure of crystallization (Cawthorn et al. 1976; Green 1978; Clark et al. 2005, 2007). Besides muscovite, cordierite, garnet and Al_2SiO_5 polymorphs or feldspars, biotite is the most important aluminium concentrator and in biotite-dominated granitoids it directly determines the peraluminosity of magma (Zen 1988; Shabani et al. 2003; Bonova et al. 2010). Several possible mechanisms have been proposed for the formation of these rocks including amphibole fractionation from less siliceous melt (Cawthorn et al. 1976), partial melting of pelitic metasediments (Green 1978), vapour phase transport of alkalies (Luth et al. 1964), secondary alteration (Heming Carmichael 1973) and magma contamination (Ewart Stipp 1968). Among these, partial melting of pelitic metasedimentary rocks has attracted significant attention. According to several workers (i.e. Miller 1985; Le Fort et al. 1987; White & Chappell 1988; Sylvester 1998; Searle et al. 2010), these rocks are believed to be derived wholly or dominantly from the partial melting of metasedimentary rocks, including pelitic rocks (meta-shales) and quartzofeldspathic psammitic rocks (meta-greywackes)

by the incongruent melting of muscovite and biotite in a process called vapour-absent melting (Watt Harley 1993; Stevens et al. 1997; Waters 2001; Taylor et al. 2010). In evolved continental crust, generated melts are felsic owing to derivation from mainly meta-pelitic source rocks or extensive melt evolution during ascent. In some orogens there is evidence for either wet melting (Harrison et al. 1998; Patiño Douce & Harris 1998; Guo & Wilson 2012) or input of mantle melts (Barbarin 1999; Soesoo 2000). In the Sanandaj-Sirjan metamorphic belt of west Iran, many granitoid bodies intruded from Jurassic to Cenozoic (e.g. Takin 1972; Berberian et al. 1982; Mohajjal et al. 2003; Agard et al. 2011; Chiu et al. 2013; Sepahi et al. 2014). Among the intrusive complexes of the central SSZ, the Marziyan granites (Fig. 1) are very poorly studied and mineral chemistry, petrologic and geochemical data on these rocks are scarce. The purpose of the work presented here is to describe the field relationships, petrography, mineral chemistry and geochemistry of the Marziyan granites, as well as discussing their petrogenetic and tectonic significance in the light of the regional framework of the Sanandaj-Sirjan Zone. The data from this study will shed light on the petrogenesis of these rocks and the mode of their emplacement.

Geological setting

The Marziyan granites are located in the north of Azna and crop out in an area between the Marziyan and the Kolbor villages which cover an area of approximately 30 km^2 , between N $33^{\circ}31'2"-33^{\circ}38'2"$ and E $49^{\circ}24'2"-49^{\circ}32'2"$. The Sanandaj-Sirjan Zone, in terms of structural framework, is known as an active geological zone in Iran (Mohajjal et al. 2003) which has

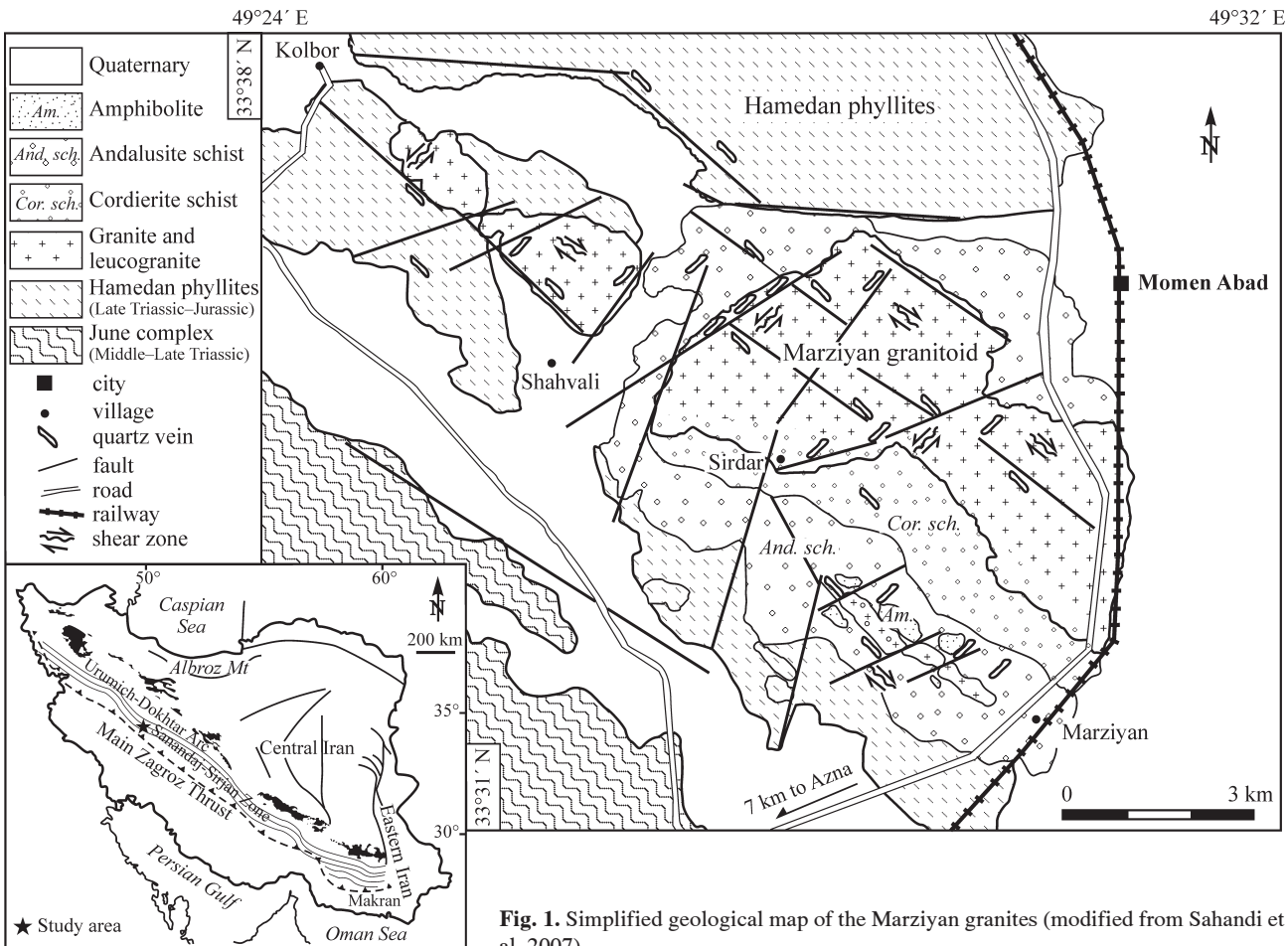


Fig. 1. Simplified geological map of the Marziyan granites (modified from Sahandi et al. 2007).

experienced different deformations, metamorphic and magmatic events since the Cenozoic time. Detailed geological data from the area under study are scarce and are mainly limited to reconnaissance reports. The Sanandaj-Sirjan Zone in the Azna area is characterized by the predominance of metamorphic rocks and the presence of several granite and leucogranitic bodies. The metamorphic rocks are composed of various meta-sedimentary assemblages from low to high metamorphic grade. The basement of the area (Fig. 1) is dominated by the pre-Jurassic, low- to very low-grade metamorphic rocks (June Complex — Mohajjal et al. 2003), such as meta-volcanic and tuffs, meta-cherty limestone, meta-sandstone, slates and phyllites (Hamedan Phyllites: Fig. 1). The intrusion of the Marziyan granites into the Hamedan Phyllites in the Late Cretaceous-Eocene (Sahandi et al. 2007) gave rise to low-grade thermal aureole (up to albite-epidote to hornblende-hornfels facies) (Fig. 2). Contact metamorphic rocks, consisting of spotted schist, andalusite-garnet schist and cordierite schist (hornfelses), are exposed only in the southern portions of the pluton. The northern margin of the complex is controlled by a fault system parallel to the contact where the granite thrust over metamorphic rocks. Thus, the traces of contact metamorphism have been obliterated. The presence of mantle-derived materials emplaced as diabasic dykes into the granites and metamorphic rocks contributed to the heat source for the partial melting of the country rocks. From a tectonic

perspective, the deformational features (i.e. fault, joints, mylonitization, schistosity and veins of the Marziyan granites) were exposed with two different trends: (a) the NW-SE trend; a compressional trend, running parallel to the main Sanandaj-Sirjan belt trend, (b) and the NE-SW trend: shear stresses after collision (Mohajjal et al. 2003). The trend of elongation in the granites studied is very similar to that of the faults and joints in the country rocks. Therefore, the Marziyan granites were likely emplaced during the major deformational event in the area. The direction of mylonitization and elongated veins is parallel to the direction of the schistosity in country rocks and corresponding roughly to the main trend of the Sanandaj-Sirjan Zone. The feature infers a syn-deformational (syn-collision) emplacement of the Marziyan granites.

Analytical methods

About two hundred rock samples were collected from localities scattered over the area of investigation. One-hundred and fifty thin sections were studied by optical microscope. For chemical analysis, approximately 1 kg of each sample was crushed into smaller chips in a steel jaw crusher. Then chips of the samples were pulverized below 200 mesh with a soft iron shatter box. Bulk major, minor and trace element analyses were conducted on 12 representative granitic samples

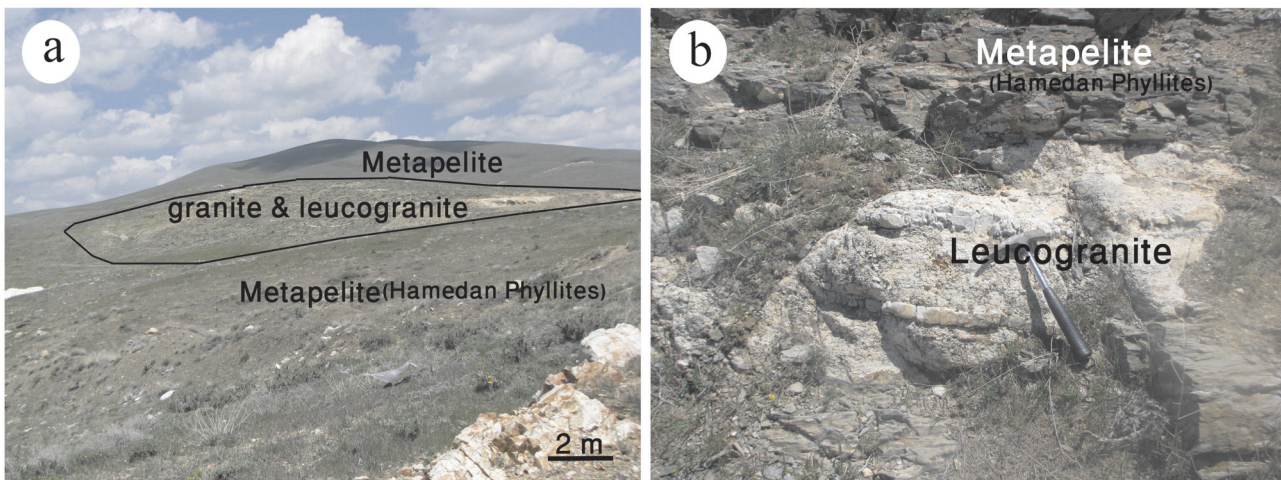


Fig. 2. Photographs showing field geological features of Marziyan granites that intruded in the metapelitic rocks.

(Table 1). Whole-rock major oxides were analysed by using X-ray fluorescence (XRF) spectrometry at the Southern Methodist University, Dallas (USA) and trace elements including rare earth elements (REE) data were acquired by Inductively Coupled Plasma-Mass Spectrometry (ICP-MS) at the Labwest Minerals Analysis Pty Ltd in Western Australia. The analyses were carried out with a detection limit of 0.01–10 ppm following lithium metaborate fusion method, using high pressure digestion in microwave apparatus including HF. The results are presented in Table 2. Major-element compositions of the biotite and muscovite minerals in selected leucogranites were determined by wave length-dispersive spectrometry using the Cameca JXA-8800 (WDS) microprobe JEOL at Russian Government University. The operational conditions were 20 kV, 12 nA specimen current. The analytical spot diameter was set between 3 and 5 mm, keeping the same current conditions. Representative mineral analyses of leucogranites are presented in Tables 3 and 4.

Petrography and field relations

Based on field studies as well as petrographic characteristics, the Marziyan granites are mainly dominated by leucogranite to granite. The most abundant and characteristic rock

type of the Marziyan pluton is leucogranite which is scattered in portions throughout the area and intruded into the metapelites (Fig. 2a,b). Small volumes of mylonitized granite are commonly present in the shear zones. The granites are mainly coarse to medium grained, white to light grey and hypidiomorphic granular (Figs. 2, 3). Mineralogically these rocks are composed of quartz, K-feldspar, and plagioclase as well as muscovite, biotite, garnet, tourmaline, minor sillimanite, apatite and small amounts of zircon and monazite (Table 1). Alteration of biotite to chlorite and of feldspar to sericite is dispersed throughout the rocks. These rocks have been variably subjected to deformation. The most deformed parts of the granite are characterized by mineral orientation and quartz recrystallization, while the undeformed parts have poikilitic K-feldspar and quartz enclosing biotite and plagioclase. Subhedral granular texture with perthitic microcline are the common petrographic features of the rocks studied. The prevailing textures of the rocks are granular porphyric, (with relatively larger K-feldspar, tourmaline and garnet crystals), and cataclastic texture (crushed minerals such as tourmaline and garnet). Most of the coarse-grained granites show subsolvus recrystallization, in terms of two separate feldspar crystallizations, containing both plagioclase and K-feldspar. Small shear zones were well developed in some portions. They are a response to regionally imposed stress. Field observations and

Table 1: Modal analyses of representative Marziyan granites (in vol. %).

Sample	Qz	Kfs	Pl	Bt	Ms	Grt	Tur	Sill	Ap	Zr	Opq
S-20	33.2	28.5	27.2	3.9	4.2	0.8	—	0.8	0.9	0.3	0.5
M-4	32.4	33.1	24.1	1.9	2.7	2.6	—	—	0.6	0.2	0.4
M-13	31.3	27.2	32.3	3.4	2.1	0.2	—	—	0.8	0.8	0.7
M-40	38.1	21.4	31.4	0.2	2.4	—	4.6	—	1	0.2	0.4
Az-2	37.2	29.2	22.4	2.5	1.7	0.4	—	—	0.4	0.3	0.6
Az-8	39.2	29.1	27.2	2.1	2.2	0.5	—	—	0.5	0.2	0.3
Az-9	39.2	22.5	27.4	4.6	1.5	—	0.4	—	0.6	0.5	0.5
Az-10	38.8	28.5	25.2	3.2	2.3	0.5	—	—	0.6	0.2	0.8
Az-24	37.8	22.6	25.1	5.1	4.4	0.9	—	0.5	0.8	0.5	0.5
Sh-4	39.2	29.6	22.2	4.4	7.5	0.7	—	—	0.7	0.4	0.9
Sh-5	41.3	30.1	24.2	3.5	2.3	—	0.2	—	0.7	0.2	0.7
Sh-9	43.2	21.1	23.2	1.4	4.5	—	0.5	—	0.8	0.4	0.5

Table 2: Representative major element (wt. %) and trace element including REE (ppm) compositions of the Marziyan granites.

Sample no.	S-20	M-4	M-13	M-40	Az-2	Az-8	Az-9	Az-10	Az-24	Sh-4	Sh-5	Sh-9
SiO ₂	69.85	71.05	70.75	71.36	73.41	74.5	71.78	72.81	70.4	72.92	73.42	77.5
Al ₂ O ₃	18.5	16.03	15.46	17.52	15.05	14.05	17.12	15.12	18.4	15.08	15.17	14.64
CaO	0.75	1.05	1.4	0.9	0.38	0.4	0.35	0.6	0.83	0.51	0.4	0.3
K ₂ O	4.38	5.98	4.6	2.9	4.5	5.12	3.1	5	3.6	5.3	5.8	3.83
Na ₂ O	4.2	2.96	3.9	5	4.3	3.95	3.9	3.5	3.9	4.1	3.1	2.74
MgO	0.26	0.2	0.7	0.26	0.3	0.2	0.98	0.45	0.4	0.25	0.2	0.45
(Fe ₂ O ₃) _{tot}	0.7	0.62	1.8	0.7	1.02	1	1.01	1.3	1.2	1.01	0.6	1.1
MnO	0.05	0.08	0.02	0.02	0.02	0.03	0.01	0.04	0.02	0.02	0.04	0.02
P ₂ O ₅	0.76	0.06	0.2	0.99	0.06	0.04	0.05	0.11	0.8	0.13	0.1	0.07
TiO ₂	0.02	0.02	0.2	0.02	0.08	0.04	0.08	0.14	0.042	0.1	0.07	0.06
L.O.I.	1.05	0.96	0.98	1	0.75	0.63	0.92	0.93	0.86	0.8	0.8	0.5
Total	100.5	99.06	100.01	100.7	99.87	99.96	99.3	100	100.5	100.2	99.76	100.98
A/CNK	1.36	1.22	1.19	1.46	1.14	1.11	1.5	1.24	1.47	1.13	1.15	1.35
A/NK	1.5	1.4	1.35	1.69	1.21	1.15	1.57	1.34	1.67	1.3	1.2	1.62
Corundum	2.4	2.1	1.2	2.1	1.8	1.1	2.8	2.1	2.9	1.4	2.1	2.6
Ba	313	527	353	332	454	342	417	475	382	428	352	338
Sr	35	187	122	47	63	32	47	90	58	58	45	35
Rb	108	198	118	148	159	341	105	188	111	213	321	216
Cs	18	12	38	45	27	25	39	24	41	36	23	36
Zr	28	40	105	35	64	76	98	86	57	81	75	71
Y	19	25	29	8	18	21	26	15	18	27	16	14
Th	14	23	24	10	25	16	12	24	11	16	12	18
Ta	1.33	0.91	3	5.36	1.99	5.6	3.1	2.5	1.92	6.3	4.04	2.55
Ga	13	13.9	16	20	19	17	20	16	15	17	19	18.5
Nb	10	15	22	21	16	20	21	19	16	24	19	21
Ni	4	4	5	4	7	4	7	5	4	4	5	4
Pb	40	20.5	16.5	24	16.7	23.9	26	19	27	29	32	21
Hf	0.44	0.87	0.55	0.35	0.77	0.55	0.88	0.86	0.57	0.94	0.82	0.97
La	12.4	23	41.5	11	15	12.9	30	18	12	23.3	33	22
Ce	22.6	45	75.6	19	27.3	21.8	56.4	34.6	20.5	41.1	62	41.2
Pr	4	4.3	7.75	3.2	9.2	5.3	9.7	7.2	5.4	4.7	4.9	5
Nd	14.2	12.2	25	13.2	16.9	17	22.4	14.5	16.3	16.4	16.6	15.4
Sm	3.4	2.92	4.2	3.1	4.32	3.42	3.3	4.6	4.9	4.64	3.1	3.55
Eu	0.17	0.76	0.9	0.18	0.39	0.44	0.56	0.26	0.29	0.21	0.47	0.36
Gd	1.67	2.99	3.56	1.9	1.9	3.1	2.2	3.4	2.98	3.5	2.3	2.68
Tb	0.38	0.81	0.79	0.34	0.55	0.36	0.29	0.46	0.59	0.66	0.59	0.58
Dy	2.1	5.28	4.9	1.9	2.86	2.55	2.6	2.9	2.21	4.8	2.24	3.4
Ho	0.47	0.98	0.88	0.44	0.52	0.46	0.51	0.49	0.54	0.91	0.58	0.54
Er	1.43	2.9	2.1	0.95	0.69	0.63	0.72	0.79	0.66	2.5	0.99	0.81
Tm	0.39	0.71	0.55	0.27	0.44	0.28	0.35	0.26	0.5	0.6	0.34	0.32
Yb	1.8	4.1	3.2	1.5	2.8	2.56	1.98	2.4	2.42	4.2	1.9	1.87
Lu	0.27	0.68	0.56	0.24	0.48	0.45	0.19	0.46	0.63	0.58	0.33	0.29
ΣREE	65.28	106.96	171.49	57.22	83.35	71.25	131.2	90.32	69.92	108.1	129.34	97.94
Rb/Sr	3.3	1.1	0.97	3.2	2.6	10.7	2.2	2.1	1.9	3.7	7.1	6.2
Rb/Ba	0.35	0.38	0.33	0.45	0.35	1	0.25	0.6	0.3	0.5	0.91	0.64
Rb/Zr	3.9	4.95	0.99	4.3	2.5	4.5	0.97	2.2	1.95	2.63	4.3	3.1
Sr/Ba	0.11	0.36	0.35	0.14	0.14	0.1	0.11	0.19	0.15	0.14	0.13	0.11
Eu/Eu*	0.22	0.79	0.71	0.23	0.34	0.41	0.64	0.20	0.23	0.16	0.54	0.36
T _{Zr} (°C)	671	688	753	684	723	731	779	748	730	735	740	755

petrographic evidence such as the occurrence of muscovite and garnet and the absence of hornblende and primary sphene, strongly support the peraluminous (S-type) nature of the Marziyan granites and an origin for these rocks derived from partial melting of crustal protolith.

Discussion

Mineral chemistry

To determine the chemical composition of biotite and muscovite in the studied samples, three fresh and representative samples from the granites under discussion were selected.

Biotite

Biotite is a significant ferromagnesian mineral in most intermediate and felsic igneous rocks, and occurs, as a minor phase in some mafic rocks. In the Marziyan granitic rocks, biotite is the dominant ferromagnesian phase. Other mafic minerals such as garnet, tourmaline, chlorite and ilmenite may occur, but only in trace amounts. Petrographically, biotites from the Marziyan granites differ in their pleochroic scheme, some being pleochroic in shades of reddish brown and some in bright fire-red (Fig. 3a,b). Representative electron microprobe analyses of the biotites from the studied rocks are displayed in Table 3. The value of Fe³⁺ is estimated by the approach of Dymek (1983). According to classifica-

Table 3: Representative electron microprobe analyses and the structural formula of biotites based on 11 atoms of oxygen.

Sample no.	Sh-4	Sh-4	Sh-4	Sh-4	S-20	S-20	S-20	S-20	Az-24	Az-24	Az-24	Az-24
SiO₂	34.85	35.31	34.35	34.65	35.2	34.5	35.9	35.2	34.98	36.02	34.78	35.4
TiO₂	2.15	1.98	2.35	2.23	1.3	1.9	0.95	1.5	1.95	0.35	2.2	1.8
Al₂O₃	17.97	18.22	17.86	18.2	18.6	18.3	19	18.1	18.1	20.46	17.36	17.53
FeO_{tot}	24.65	24.44	24.75	25.12	24.2	24	24.5	25	24.96	23.39	24.67	25.31
MnO	0.75	0.54	0.68	0.66	0.37	0.35	0.39	0.45	0.62	0.22	0.63	0.63
MgO	6.18	6.12	6.24	6.52	6.2	6.1	6.2	5.9	6.38	6.3	6.34	6.47
CaO	0.15	0.21	0.13	0.14	0.22	0.24	0.21	0.14	0.14	0.33	0.13	0.13
Na₂O	0.02	0.01	0.07	0.03	0.04	0.02	0.06	0.02	0.05	0.09	0.1	0.01
K₂O	9.64	9.15	9.35	9.58	9.2	9.65	8.9	9.45	9.51	6.4	9.47	9.55
Total oxide	96.36	95.98	95.75	97.13	95.33	95.06	96.11	95.76	96.69	93.56	95.68	96.83
Si	2.68	2.71	2.66	2.65	2.71	2.68	2.74	2.72	2.68	2.75	2.70	2.71
Al^{IV}	1.32	1.29	1.34	1.35	1.29	1.32	1.26	1.28	1.32	1.25	1.30	1.29
Al^{VI}	0.31	0.36	0.29	0.29	0.41	0.36	0.44	0.36	0.32	0.60	0.28	0.30
Ti	0.12	0.11	0.14	0.13	0.08	0.11	0.05	0.09	0.11	0.02	0.13	0.10
Fe²⁺	1.55	1.56	1.51	1.51	1.51	1.51	1.52	1.56	1.56	1.45	1.55	1.59
Fe³⁺	0.03	0.00	0.09	0.09	0.05	0.05	0.05	0.05	0.04	0.04	0.05	0.03
Mn	0.05	0.04	0.04	0.04	0.02	0.02	0.03	0.03	0.04	0.01	0.04	0.04
Mg	0.71	0.70	0.72	0.74	0.71	0.71	0.70	0.68	0.73	0.72	0.73	0.74
Ca	0.01	0.02	0.01	0.01	0.02	0.02	0.02	0.01	0.01	0.03	0.01	0.01
Na	0.00	0.00	0.01	0.00	0.01	0.00	0.01	0.00	0.01	0.01	0.02	0.00
K	0.95	0.90	0.92	0.93	0.90	0.96	0.87	0.93	0.93	0.62	0.94	0.93
Total	9.73	9.67	9.73	9.75	9.69	9.72	9.67	9.71	9.73	9.51	9.73	9.73
Mg/Mg+Fe	0.31	0.31	0.31	0.32	0.31	0.31	0.31	0.30	0.31	0.32	0.31	0.31

Table 4: Representative electron microprobe analyses and the structural formula of white micas based on 11 atoms of oxygen.

Sample no.	Sh-4	Sh-4	Sh-4	Sh-4	S-20	S-20	S-20	S-20	Az-24	Az-24	Az-24
SiO₂	45.12	44.89	45.5	46.1	45.8	46.5	47	6.11	45	46.13	
TiO₂	1.08	1.12	1.03	1.01	1.05	0.9	0.9	0.02	0.09	0.01	
Al₂O₃	35.05	34.87	35.8	35.9	35.7	35.5	34.2	35.95	38.31	34.61	
FeO_{tot}	1.82	1.76	1.92	1.99	1.89	2.45	1.9	2.61	1.08	2.28	
MnO	0.06	0.05	0.07	0.07	0.07	0.09	0.01	0.08	0.01	0.01	
MgO	0.36	0.24	0.28	0.35	0.25	0.49	0.49	0.47	0.11	0.98	
CaO	0.05	0.05	0.04	0.04	0.04	0.03	0.01	0.09	0.11	0.07	
Na₂O	0.32	0.42	0.39	0.37	0.41	0.3	0.4	0.25	0.29	0.16	
K₂O	11.1	11.08	11.03	11.01	11.05	10.25	10.9	10.38	11.26	11.36	
Total oxide	94.96	94.48	96.06	96.84	96.26	96.51	95.81	95.96	96.26	95.61	
Si	3.04	3.04	3.03	3.04	3.04	3.07	3.12	3.06	2.97	3.09	
Al^{IV}	0.96	0.96	0.97	0.96	0.96	0.93	0.88	0.94	1.03	0.91	
Al^{VI}	1.82	1.82	1.83	1.83	1.83	1.82	1.80	1.87	1.96	1.82	
Ti	0.05	0.06	0.05	0.05	0.05	0.04	0.04	0.00	0.00	0.00	
Fe²⁺	0.10	0.10	0.11	0.11	0.10	0.14	0.11	0.14	0.06	0.13	
Fe³⁺	0.00	0.00	0.00	0.00	0.00	0.00	0.00	0.00	0.00	0.00	
Mn	0.00	0.00	0.00	0.00	0.00	0.01	0.00	0.00	0.00	0.00	
Mg	0.04	0.02	0.03	0.03	0.02	0.05	0.05	0.05	0.01	0.10	
Ca	0.00	0.00	0.00	0.00	0.00	0.00	0.00	0.01	0.01	0.01	
Na	0.04	0.06	0.05	0.05	0.05	0.04	0.05	0.03	0.04	0.02	
K	0.95	0.96	0.94	0.93	0.94	0.86	0.92	0.88	0.95	0.97	
Total	9.01	9.02	9.01	9.00	9.01	8.96	8.98	8.99	9.02	9.04	
Mg/Mg+Fe	0.26	0.20	0.21	0.24	0.19	0.26	0.31	0.24	0.15	0.43	

tion of Deer's (1996, 2001) diagram, the biotites of the Marziyan pluton are classified as Fe-rich biotite (siderophyllitic) (Fig. 4). The Fe/(Fe+Mg) ratio in these phases is about 0.68. Nachit (1986) used mica composition in granitoids to relate the magma types in which biotite crystallized. In the Al (total) vs. Mg classification diagram, the nature of granitic magmas was grouped into four types such as peraluminous, calc-alkaline, sub-alkaline, and alkaline-peralkaline (Fig. 5a). Biotites from the Marziyan granites are clustered in the peraluminous field (Fig. 5a). Igneous biotites can also provide valuable petrogenetic information. Three general reviews on

micas in igneous rocks are provided by Foster (1960) and Speer (1984). Biotite specimens in granitic rocks show that the chemical composition and the colour of this mineral strongly reflect the tectonic origin of its host (Lalonde & Bernard 1993). In the continental collision-related granites, biotite is enriched in total Al and Fe and is Fe³⁺-poor, consistent with anatexis or assimilation of a reduced metasedimentary material. The bright red colour of biotite from peraluminous collisional granitic plutons reflects a high total Fe content with low Fe³⁺/(Fe²⁺+Fe³⁺), and probably also the presence of Ti³⁺. Trying to use biotite's capability to deter-

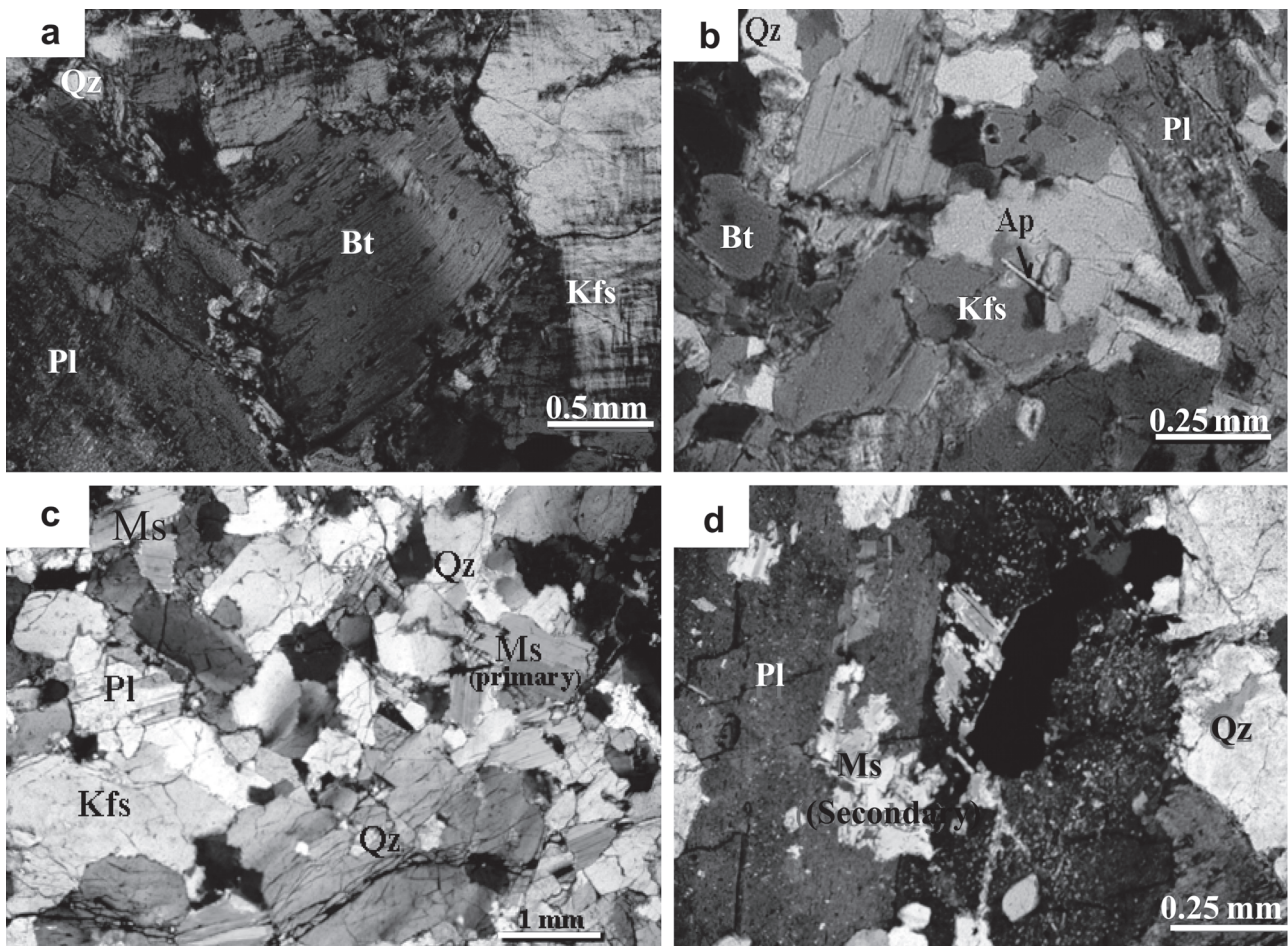


Fig. 3. Photomicrographs of representative samples from the Marziyan granites, (crossed nicols). **a** — the granites displaying subhedral granular quartz with biotites, orthoclase, plagioclase; **b** — leucogranite containing biotite phenocrysts; **c** — muscovite granite containing primary muscovite, quartz, plagioclase and K-feldspar granite; **d** — secondary muscovite with plagioclase. **Qz** — quartz, **Bt** — biotite, **Pl** — plagioclase, **Ms** — muscovite, **Kfs** — K-feldspar (abbreviations from Whitney & Evans 2010).

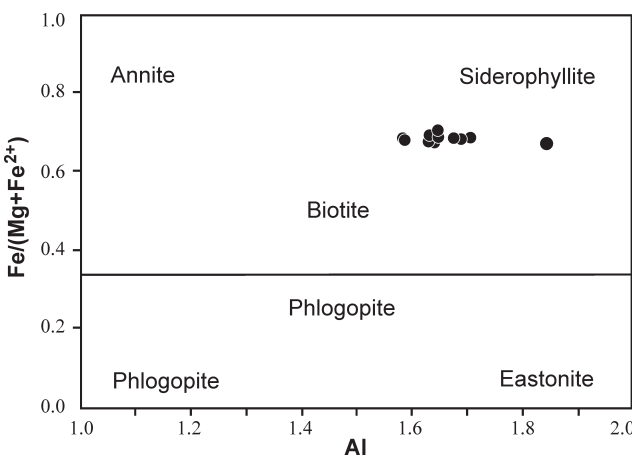


Fig. 4. Diagram of Deer et al. (1996) indicates that analysed biotites are siderophyllite.

mine the magmatic series, Abdel-Rahman (1994) introduced four efficient diagrams discriminating alkaline, calc-alkaline and peraluminous (including S-type) natures. These diagrams

identifying magmatic nature based on biotite chemistry for the Marziyan granitic rocks are presented in Fig. 5b,c,d,e. These diagrams clearly show that the parent magma of analysed biotites had peraluminous nature (Fig. 5b,c,d,e). Biotite is also a very useful and suitable indicator of the oxidation-reduction state in a melt (Wones & Eugster 1965; Burkhard 1993; Bonova et al. 2010). Biotites from the Marziyan granites have a FeO^*/MgO ratio of 3–4, low TiO_2 and high Al_2O_3 (Fig. 6a), on the basis of this diagram all the studied samples are plotted in ilmenite series (Ishihara 1977) indicating a reducing environment for the granites under discussion (Karimpour et al. 2011). The Ti content of biotite is believed to be dependent on the temperature of crystallization of biotite and the oxygen fugacity ($f\text{O}_2$) (Henry et al. 2005) and possibly on the volatile content of the magma. Low Ti content correlates with low temperature of crystallization and low oxygen fugacity (Henry et al. 2005). High Al_2O_3 and low TiO_2 values in the biotites of the area reflect geochemical features characteristic of ilmenite series of granites (Fig. 6a,b). Biotites with high Al concentrations seem to be characteristic of peraluminous granites (e.g. Clarke et al. 2005; Dahlquist et al. 2007) where they coexist with alumini-

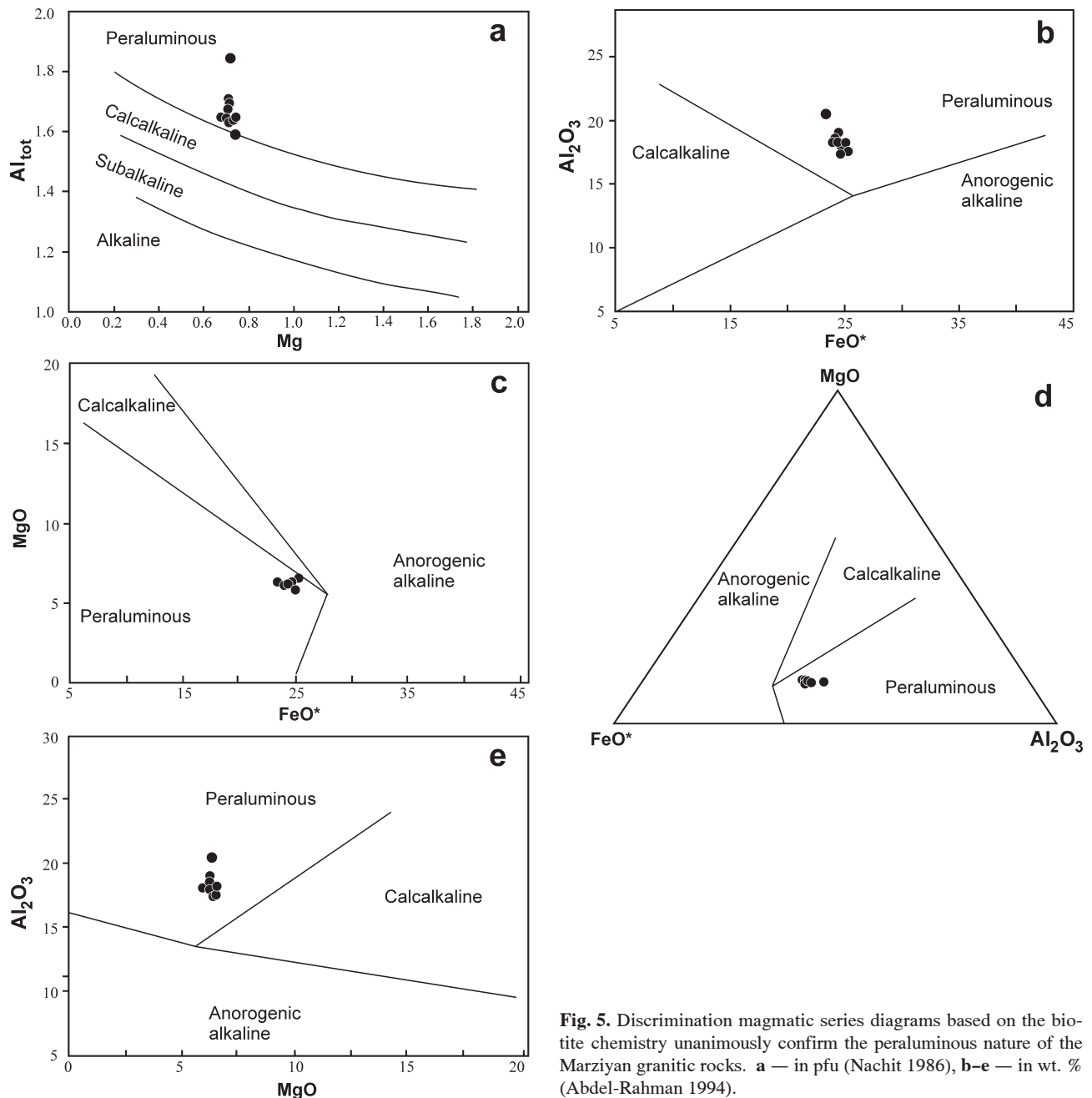


Fig. 5. Discrimination magmatic series diagrams based on the biotite chemistry unanimously confirm the peraluminous nature of the Marziyan granitic rocks. **a** — in pfu (Nachit 1986), **b–e** — in wt. % (Abdel-Rahman 1994).

nous minerals. However, the most commonly invoked process, and probably the one responsible for the bulk of peraluminous granites, is anatexis or assimilation of pelitic metasediments (Chappell & White 1987). In the Marziyan granites, biotites are enriched in total Al and Fe contents and are consistent with anatexis or assimilation of a reduced metasedimentary material. In the Fe^{2+} - Fe^{3+} - Mg diagram of Wones & Eugster (1965), biotite composition from the Marziyan granites defines a cluster falling on the quartz-fayalite-magnetite (QFM) oxygen fugacity buffer (Fig. 6b). A better evaluation of oxygen fugacity can be made from the $\text{Fe}/(\text{Fe}+\text{Mg})$ ratio of the biotite by using the calibrated curves of Wones & Eugster (1965) and Wones (1989) buffer (ilmenite granites).

White mica

Two types of white mica (muscovite) are distinguished in the samples studied: large euhedral to subhedral flakes white mica and small flakes of secondary white mica unevenly dispersed in feldspar, rarely in biotite (Fig. 3c,d). The secondary white mica contains less Mg, Fe, Ti and more Al (Fig. 7a). The morphology of the primary white mica flakes; their relationships to other rock-forming minerals, as well as systematic compositional difference from the secondary white mica suggest a magmatic origin of the primary white mica (Fig. 3c,d). According to the classification of micas into 6 end-members (Dymek 1983), the analysed white micas are mostly represented by muscovite. White mica is the other sheet silicate

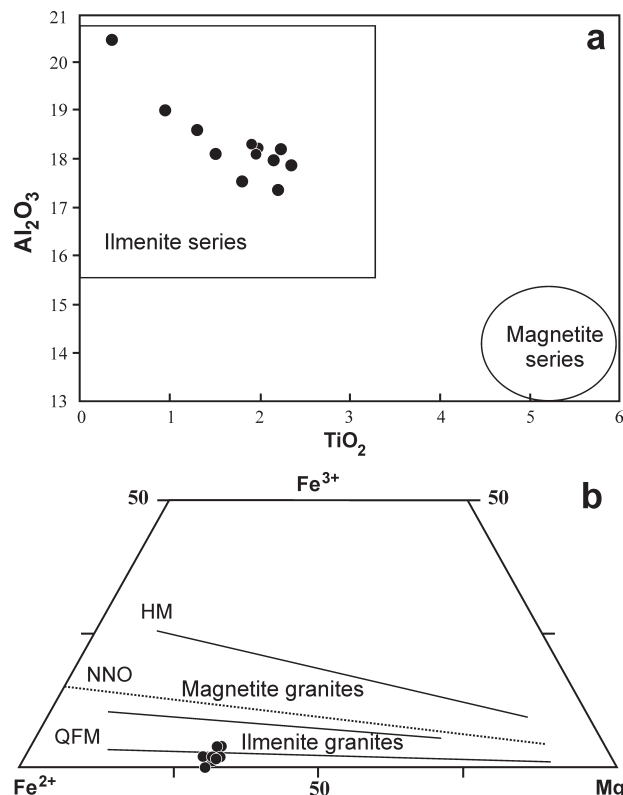
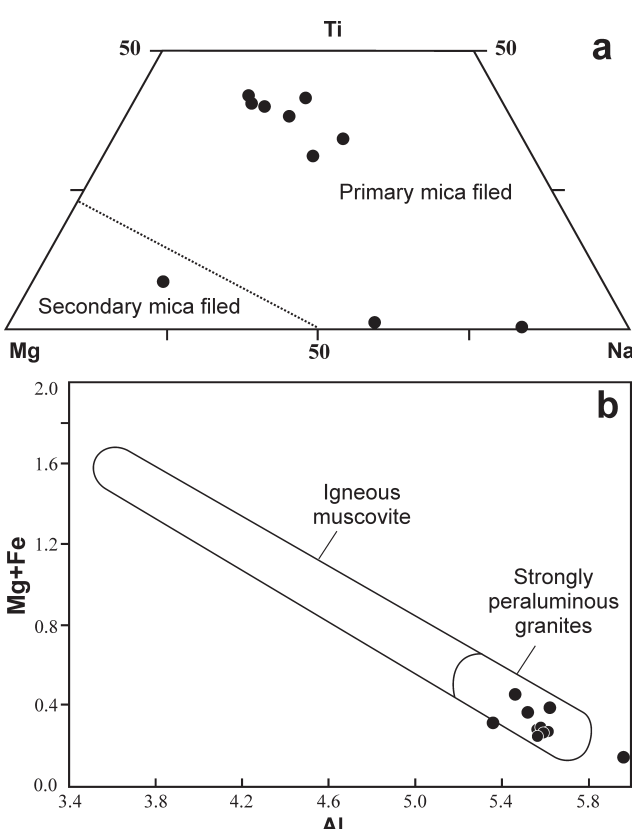


Fig. 6. a — Al_2O_3 - TiO_2 diagram after Karimpour et al. (2011), b — Fe^{2+} - Fe^{3+} - Mg diagram of Wones & Eugster (1965). Biotites from the Marziyan granites cluster near the QFM and ilmenite series.



present. Care was taken to determine whether it is of primary or secondary origin, since primary white mica is widely held to be an indicator of peraluminous magmas (Speer 1984). Petrographic observations using the criteria of Miller et al. (1981) suggest that both types of white mica are present in the studied samples. Chemical analyses were made of presumed primary white micas (Table 4), which fall in the appropriate field of the Mg - Ti - Na diagram (Fig. 7a) according to the division established by Miller et al. (1981). The analysed white mica, according to classification of micas into 6 end-members (Dymek 1983), are mostly composed of muscovite. As Fig. 7b (Zane & Rizzo 1999), displays, the Marziyan samples fall in the strongly peraluminous muscovite component field. They are also distinctively Fe-rich, similar to those in typical S-type granite and those reported by Clarke et al. (2005) as coexisting with aluminous minerals. Thus, both textural and chemical evidence indicates a primary origin for almost all the studied white mica. The petrographic and compositional characteristics of the Fe-rich white mica in the Marziyan granites (Fig. 7b) indicate an origin by crystallization of primary muscovite from a peraluminous magma (Miller et al. 1981; Clarke et al. 2005; Dahlquist et al. 2007).

Whole-rock geochemistry

Major element data

The chemical compositions of the Marziyan granites are reported in Table 1. The SiO_2 contents of the representative samples vary from 69.85 to over 77.5 wt. % CaO . The high alumina content (Al_2O_3 : 14.05–18.5 %) relative to alkalis (Na_2O : 2.7–5 % and K_2O : 2.9–5.98 %) and calcium (CaO : 0.3–1.44 %) is reflected in a high percentage of normative corundum and a high molecular ratio $\text{Al}_2\text{O}_3/(\text{CaO}+\text{Na}_2\text{O}+\text{K}_2\text{O})$ (A/CNK) (Fig. 8a). These rocks with low $\text{TiO}_2+\text{Fe}_2\text{O}_{3(\text{tot})}+\text{MgO}$ (0.76–2.53) can be classified as leucogranites. In the ternary Ab-An-Or normative diagram (Barker 1979), the Marziyan granitic rocks are classified as granite (Fig. 8b) and on the MALI ($\text{Na}_2\text{O}+\text{K}_2\text{O}-\text{CaO}$) vs. SiO_2 diagram (Frost & Frost 2008) they fall in both granite and granodiorite fields (Fig. 9a). Incidentally, samples with low FeO_{tot} display broadly magnesian character (Fig. 9b).

Trace element data

The Rb, Sr and Ba contents vary between 108–341, 32–187 and 313–527 ppm, respectively. The rocks with high Rb but lower Zr, Sr and Ba are characterized by high Rb/Zr (about 3), $\text{Rb}/\text{Ba} (>0.25)$ and Rb/Sr (0.97–10.7) ratios. The Marziyan granites show strong enrichment in alkalis and

Fig. 7. a — Composition of white micas in the triangular diagram Mg , Ti , Na (data from Table 4). The limit between fields for secondary and primary micas is from Miller et al. (1981). Main inset shows representative primary and secondary white micas in Marziyan granite filled circles; b — Chemical compositions of muscovite plotted on $\text{Mg}+\text{Fe}$ - Al diagram showing strongly peraluminous and muscovite component for Marziyan samples (Zane & Rizzo 1999).

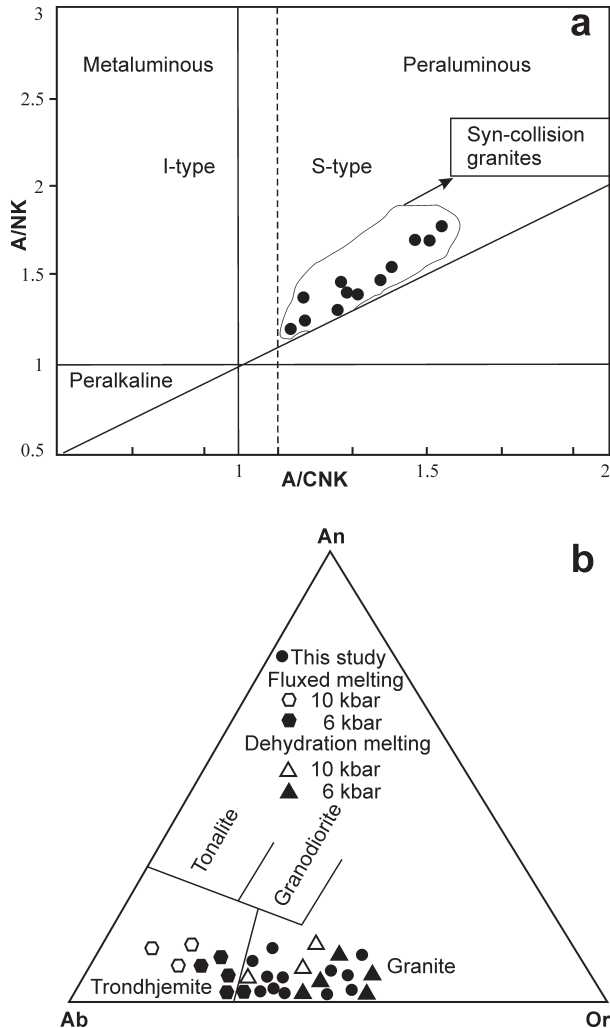


Fig. 8. a — A/NK-A/CNK diagram (Maniar & Piccoli 1989). A/NK = molar ratio of $\text{Al}_2\text{O}_3/[\text{K}_2\text{O} + \text{Na}_2\text{O}]$; A/CNK = molar ratio of $\text{Al}_2\text{O}_3/[\text{CaO} + \text{K}_2\text{O} + \text{Na}_2\text{O}]$; b — Normative albite (Ab)-anorthite (An)-orthoclase (Or) contents of the Marziyan granites, compared with experimentally generated melt compositions from metapelitic from the Himalayan belt (Patiño Douce & Harris 1998). The Ab-An-Or classification for silicic rocks follows Barker (1979).

depletion in HFS elements (Fig. 10, Table 1). Low Zr values of the rocks (28–105 ppm) are accompanied by low CaO contents of the rocks (0.3–1.44). Spider diagrams for the Marziyan granites, relative to primitive mantle (Fig. 10b), are characterized by distinct negative anomalies for Nb, Sr, P and Ti typical for upper crustal compositions (Rollinson 1993). Rb, Ba and Eu concentrations in the granites studied are variable and suggest variations in the proportions of feldspar and mica retained in the residua. La and Ce concentrations vary between 11–41.5 and 19–75.6 ppm, respectively. The studied samples are enriched in LREE relative to HREE (Fig. 11a). The Marziyan granites are characterized by negative Eu anomaly and $\text{Eu}/\text{Eu}^*(0.16–0.79)$ (Fig. 10a). Primitive mantle normalized trace element spider diagrams show (Fig. 10b) relatively high Cs, Rb, K, Th, U, Ba contents and low Sr, Ti. The REE content varies between 58.22 and

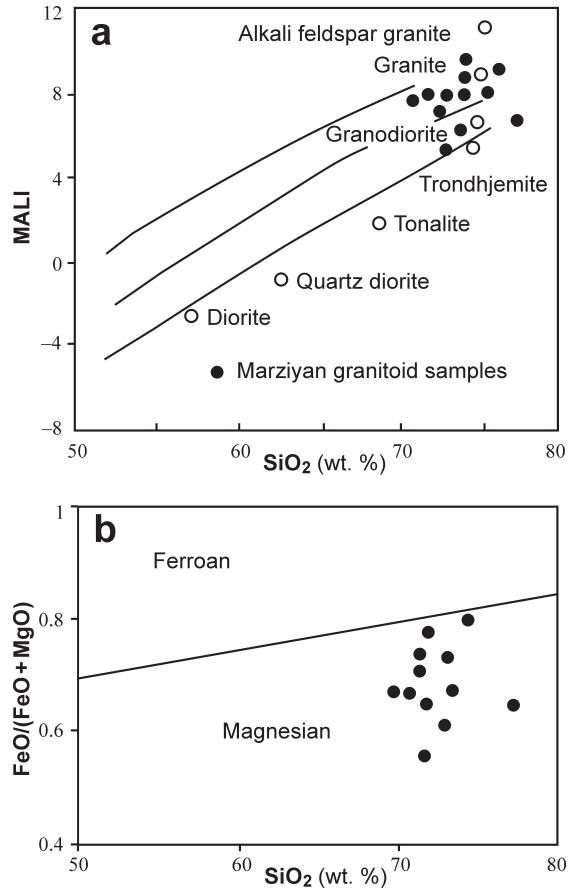


Fig. 9. Most of the Marziyan samples are located in the granite and granodiorite areas on the MALI vs. SiO_2 diagram (a) and all have magnesian character according to $\text{FeO}_{\text{tot}}/(\text{FeO}_{\text{tot}} + \text{MgO})$ vs. SiO_2 diagram (b). (Frost & Frost 2008).

171.49 ppm. REE-normalized patterns are distinctly more enriched and fractionated for LREE [$(\text{La}/\text{Sm})_{\text{N}} = 2.29–6.70$] than for HREE [$(\text{Gd}/\text{Yb})_{\text{N}} = 0.6–1.16$].

Petrology

Peraluminous leucocratic granites commonly make up relatively small syn-collision to post-collision plutons (Le Fort et al. 1987; Nabelek et al. 1992; Inger & Harris 1993). They include two-mica and muscovite-garnet granites and do not contain low-pressure, high-temperature mafic aluminous minerals (e.g. cordierite) and aluminosilicates, which are remarkable features of strongly peraluminous S-type granites (Chappell & White 1974). Comparison of the Marziyan granites with typical peraluminous leucocratic granites demonstrates significant similarities in their geological, mineralogical, mineral-chemistry and chemical properties. The presence of primary muscovite, siderophyllite biotite, garnet, tourmaline and minor sillimanite as well as the Na/K relationship and high molar A/CNK ratio can be used to infer the S-type character of the Marziyan granites (Fig. 8a). Moreover, the studied rocks with La_{N} (68), Yb_{N} (9.96) and strong negative Eu anomaly are clearly consistent with the values of these elements in S-type leucogranites ($\text{La}_{\text{N}} < 100$, $\text{Yb}_{\text{N}} < 10$,

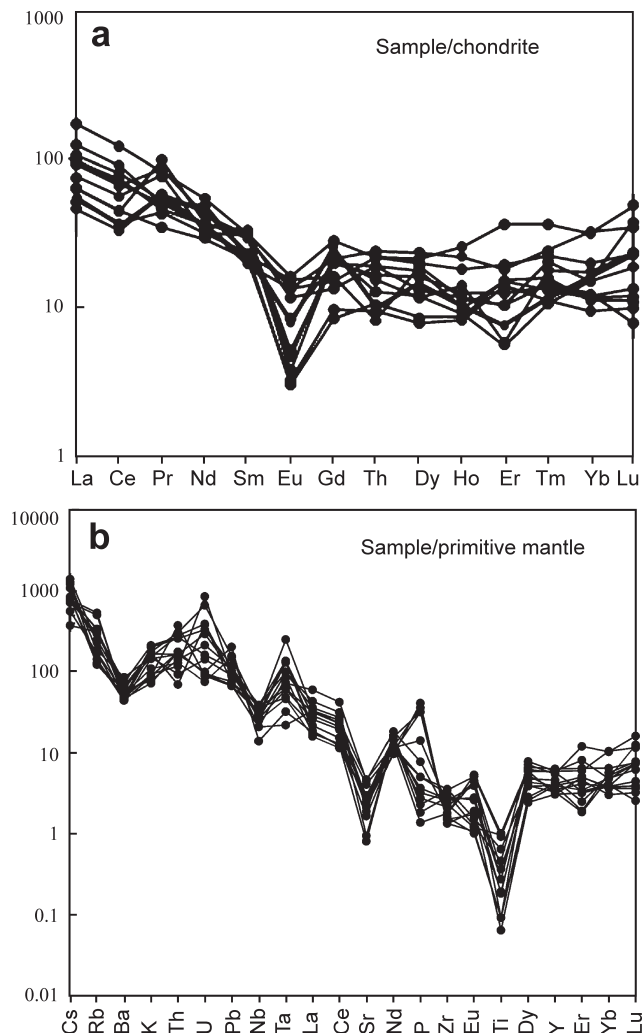


Fig. 10. a — Chondrite-normalized whole rock REE patterns for the Marziyan Granites. The chondrite values are from Boyton (1984); b — Primitive mantle-normalized trace element diagrams. Normalization factors are from Sun & McDonough (1989).

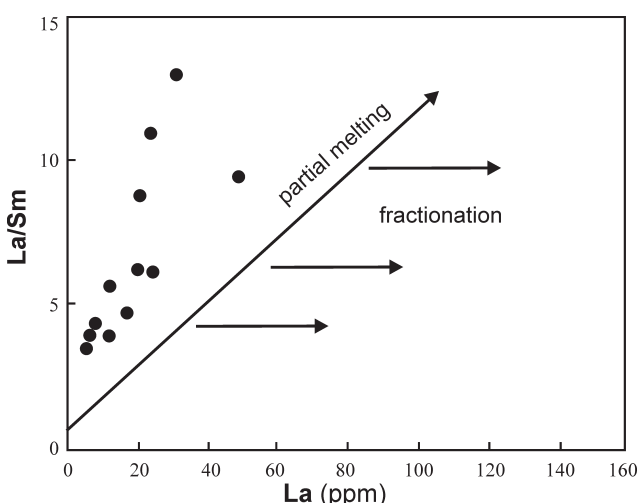


Fig. 11. La/Sm-La diagrams (Jiang et al. 2005) for the Marziyan Granites signify the partial melting for the evolution of magma.

$\text{Eu}/\text{Eu}^*<0.5$) (Williamson et al. 1996). Strong negative Eu anomaly, as Cullers & Graf (1984) cited, may be related to early fractionation of feldspar and/or melting of igneous source rocks with negative Eu anomalies, or vapour-absent melting masking the uncertainties of the feldspar/melt distribution coefficient for Eu (Harris & Igner 1992). As the Marziyan granitic samples on the La/Sm-La diagram exhibit (Fig. 11), these trace elements are more likely to be controlled by partial melting rather than fractional crystallization. On Rb/Ba vs. Rb/Sr diagram (Sylvester 1998), the majority of the Marziyan samples as well as the Himalayan granites are plotted in clay-rich sources and the lower plagioclase content field (Fig. 12b). High Rb/Sr (>0.97), medium to high Rb/Ba (>0.25) and low Sr/Ba (<0.36) ratios of the Marziyan rocks as well as low CaO, high K₂O and high Rb abundances imply metapelitic source rock melted in water-undersaturated conditions as proposed by Harris & Igner (1992) and McDermott et al. (1996). Due to involvement of plagioclase, wet melting tends to generate a rather calcic melt, whereas melts originated during dehydration melting, owing to involvement of only micas, have more alkali composition (Patiño Douce & Beard 1995). The melting with added H₂O will increase the CaO/Na₂O ratios (0.1–0.36) of peraluminous granites (Holtz & Johannes 1991). The role of muscovite (or biotite) -breakdown in the source should be apparent from strong peraluminosity (Whitney 1988). On this account, the Hamedan phyllites, in the Sanandaj-Sirjan metamorphic belt, can be regarded as the potential parental materials for the Marziyan granites. The low CaO/Na₂O in these rocks could be the result of melting without H₂O in the parental sediments (e.g. Patiño Douce & Johnston 1991; Patiño Douce & Beard 1995; Sylvester 1998). According to Villaseca et al. (2009) the S-type leucogranites, and their source rocks, are commonly depleted in REE and other “incompatible” elements (i.e. Zr, Hf and Y), relative to what would be predicted from the source composition. The low CaO and high SiO₂ contents of the Marziyan granitic rocks accompanied by low Zr values (28–105 ppm) point to the low degree of partial melting of the source. These data overlap with those of Himalayan S-type leucogranites presented by Harris et al. (1990). S-type granites commonly characterized by low Zr content (<100 ppm; e.g. Scaillet et al. 1990) because of low solubility of zircon in peraluminous melts forming at relatively low (<800) temperature (Watson & Harrison 1983). In the Ab-An-Or normative diagram (Fig. 8b), the studied granitic samples lie in the granite field and close to the composition of melts generated by dehydration melting of muscovite schist at 6 to 10 kbar (Patiño Douce & Harris 1998). Different reactions have been proposed for melting of continental crust: (a) vapour/fluid present incongruent melting of muscovite at temperature of about 700–800 °C (Thompson 1982); (b) vapour absent incongruent melting of muscovite at approximately 700–750 °C (Harris et al. 1995); (c) fluid-absent melting of biotite after dehydration of muscovite at temperatures >750 °C (Le Breton & Thompson 1988). All the mineralogical and geochemical criteria are in favour of the generation of Marziyan granites by fluid-absent melting at temperatures of about 700 °C to 800 °C and 6–10 kbars (Fig. 8b) during adiabatic

decompression or shear heating, and are solely the result of the breakdown of muscovite or biotite. Goswami et al. (2009) and Bikramaditya et al. (2011) proposed that about 10 % leucogranite melts can be generated by fluid-absent decompression melting of pelitic sediments at a temperature of around 750 °C and a pressure of 6 to 10 kbar. On the basis of zircon saturation (Watson & Harrison 1983), the Marziyan granites should have originated at approximately 750 °C (Table 1) which is not sufficient to cross the biotite break-

down reaction (Goswami et al. 2009; Bikramaditya et al. 2011), more likely in a continent-continent collision setting by partial melting of mid to upper crustal sediments (Figs. 12, 13). In the opinion of Paul et al. (2010) crustal thickening in the Sanandaj Sirjan Zone was extreme >50 km. On this account, thermal gradient has increased during collision of the Afro-Arabian and Central Iranian plates and the intrusion of Marziyan granitic rocks probably occurred by partial melting of mid to upper crustal sediments and ascended diapirically owing to their lower density and existence in a compressional environment by a shear zone.

Conclusion

On the basis of field, mineralogical and chemical features the Marziyan granites are S-type granites. These rocks consist of quartz, K-feldspar, plagioclase, biotite and Al-rich minerals (such as muscovite, garnet and minor sillimanite). The biotites from the Marziyan granites are Fe-rich (siderophyllite), with low TiO₂, high Al₂O₃, and low MgO, suggests considerable Al concentration in the source magma. These biotites were crystallized from peraluminous S-type granitic magma belonging to ilmenite series. The white micas are alumina enriched and have muscovite composition. The peraluminous composition of these rocks is shown by their high content of normative corundum (2.05), their high molar A/CNK > 1.1 ratio and the occasional presence of Al-silicate minerals (i.e. garnet, muscovite). The geochemical behaviour of some major and trace elements including their remarkably low CaO contents, CaO/Na₂O ratios (0.1–0.36) and negative Eu anomalies (0.44) generally serve as useful keys to conclude that the melts must have originated under vapour-absent conditions from a metapelitic source. The Marziyan granites display geochemical characteristics that span the medium to high K and calc-alkaline series and the

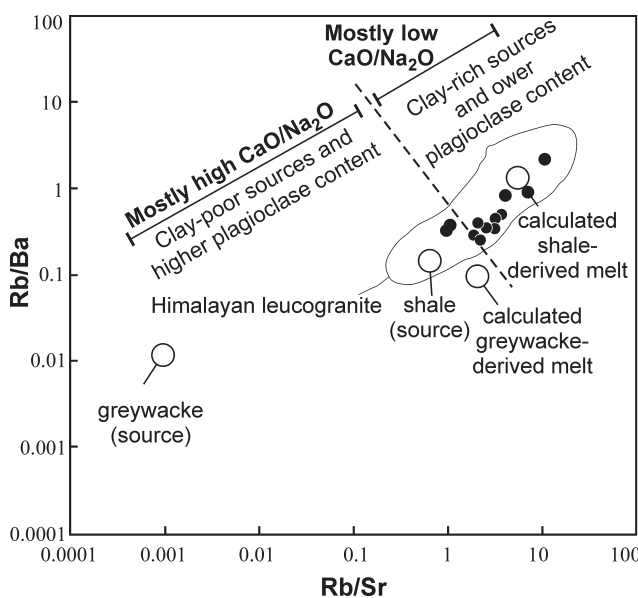


Fig. 12. a — Molar $\text{Al}_2\text{O}_3/(\text{MgO}+\text{FeOD})$ vs. molar $\text{CaO}/(\text{MgO}+\text{FeOD})$ for determining the composition of partial melts obtained by dehydration melting of various bulk compositions (Patiño Douce 1999); **b** — Rb/Ba vs. Rb/Sr diagram from Sylvester (1998). Most Marziyan samples plot in Clay-rich Sources and lower plagioclase content field same Himalayan granites field.

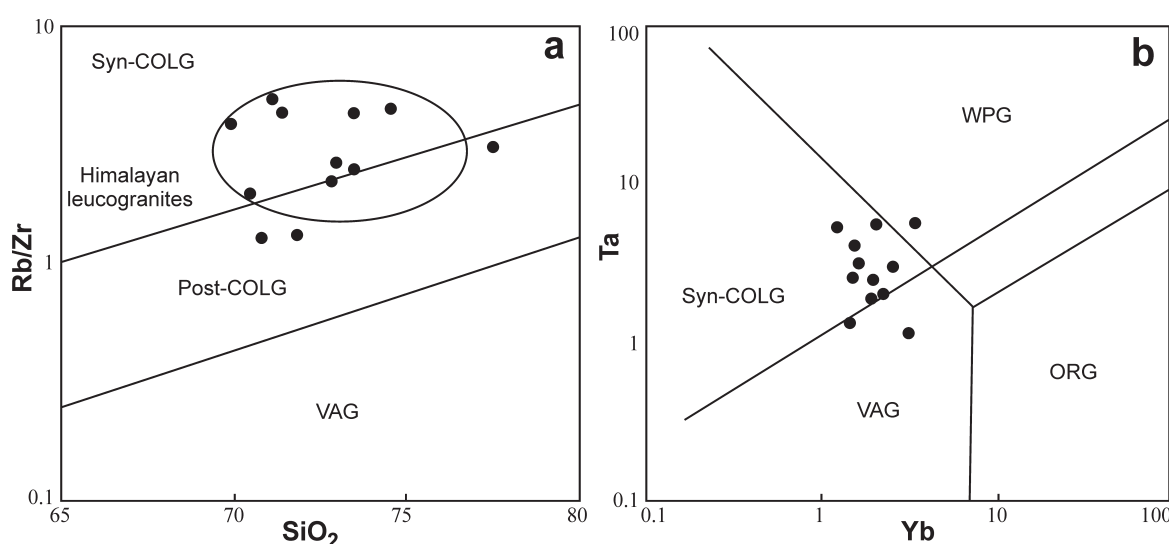


Fig. 13. a — Rb/Zr vs. SiO_2 discrimination diagram (Harris et al. 1986); **b** — Ta vs. Yb diagram (Pearce et al. 1984) for the Marziyan Granites. Note that all samples of the Marziyan plot in the Syn-COLG field and same the Himalayan granites. **VAG** — volcanic arc granite, **WPG** — within plate granite, **ORG** — oceanic related granite, **Syn-COLG** — syn-collision granite, **Post-COLG** — post collision granite.

principal features of syn-collisional magmatic intrusions related to an active continental margin. In the light of existing data and on the basis of our observation, the origin of the Marziyan granites, might have taken place in the course of the collision of the Afro-Arabian continental plate and the Central Iranian microplate.

Acknowledgment: The authors would like to thank Dr Mohsen Tabatabai Manesh for conducting microprobe analyses at the Russian Government University. Financial support of the University of Isfahan is highly acknowledged. The authors are also very grateful to the reviewers for their constructive reviews and suggestions that greatly improved the manuscript.

References

- Abdel-Rahman A.M. 1994: Nature of biotites from alkaline, calc-alkaline, and peraluminous magmas. *J. Petrology* 35, 525–541.
- Agard P., Omrani J., Jolivet L., Whitechurch H., Vrielynck B., Spakman W., Monie P., Meyer B. & Wortel R. 2011: Zagros orogeny: a subduction-dominated process. *Geol. Mag.* 148, 692–725.
- Barbarin B. 1999: A review of the relationships between granitoid types, their origins and their geodynamic environments. *Lithos* 46, 605–626.
- Barker F. 1979: Trondhjemites, dacites and related rocks. *Developments in Petrology* 6; Elsevier, Amsterdam, 1–676.
- Berberian F., Muir I.D., Pankhurst R.J. & Berberian M. 1982: Late Cretaceous and early Miocene Andean type plutonic activity in northern Makran and Central Iran. *J. Geol. Soc. London* 139, 605–614.
- Bikramaditya Singh R.K. & Gururajan N.S. 2011: Microstructures in quartz and feldspars of the Bomdila Gneiss from western Arunachal Himalaya, Northeast India: Implications for the geotectonic evolution of the Bomdila mylonitic zone. *J. Asian Earth Sci.* 42, 1163–117.
- Boynton W.V. 1984: Geochemistry of the rare earth elements: meteorite studies. In: Henderson P. (Ed.): Rare earth element geochemistry. Elsevier, 63–114.
- Bónová K., Broska I. & Petrik I. 2010: Biotite from Čierna hora Mountains granitoids (Western Carpathians, Slovakia) and estimation of water contents in granitoid melts. *Geol. Carpathica* 61, 3–17.
- Burkhard D.J.M. 1993: Biotite crystallization temperatures and redox states in granitic rocks as indicator for tectonic setting. *Geol. En. Mijnb.* 71, 337–349.
- Cawthorn R.G. 1976: Some chemical controls on igneous amphibole compositions. *Geochim. Cosmochim. Acta* 40, 1319–1328.
- Chappell B.W. & White A.J.R. 1974: Two contrasting granite types. *Pacific Geology* 8, 173–174.
- Chappell B.W. & White A.J.R. 1984: I- and S-type granites in the Lachlan Fold Belt, southeastern Australia. In: Keqin X. & Guangchi T. (Eds.): Geology of granites and their metallogenetic relations. Science Press, Beijing, 87–101.
- Chappell B.W., White A.J.R. & Wyborn D. 1987: The importance of residual source material (restite) in granite petrogenesis. *J. Petrology* 28, 1111–1138.
- Chi H., Chung S., Zarrinkoub M.H., Mohammadi S., Khatib M. & Iizuka U. 2013: Zircon U-Pb age constraints from Iran on the magmatic evolution related to Neotethyan subduction and Zagros orogeny. *Lithos* 162–163, 70–87.
- Clarke G.L., White R.W., Lui S., Fitzherbert J.A. & Pearson N.J. 2007: Contrasting behaviour of rare earth and major elements during partial melting in granulite facies migmatites, Wuluma Hills, Arunta Block, Australia. *J. Metamorph. Geology* 25, 1–18.
- Clarke D.B., Dorais M., Barbarin B., Barker D., Cesare B., Clarke G., el Baghdadi M., Erdmann S., Förster H.J., Gaeta M., Gottemann B., Jamieson R.A., Kontak D.J., Koller F., Gomes C.L., London D., Morgan VI. G.B., Neves L.J.P.F., Pattison D.R.M., Pereira A.J.S.C., Pichavant M., Rapela C.W., Renno A.D., Richards S., Roberts M., Rottura A., Saavedra J., Sial A.N., Toselli A.J., Ugidos J.M., Uher P., Villaseca C., Visonà D., Whitney D.L., Williamson B. & Woodard H.H. 2005: Occurrence and origin of andalusite in peraluminous felsic igneous rocks. *J. Petrology* 46, 441–472.
- Cullers R.L. & Graf J.L. 1984: Rare earth elements in igneous rocks of the continental crust: intermediate and silicic rocks ore petrogenesis. In: Henderson P. (Ed.): Rare earth elements geochemistry. Elsevier, Amsterdam, 275–316.
- Dahlquist J.A., Galindo C., Pankhurst R.J., Rapela C.W., Alasino P.H., Saavedra J. & Fanning C.M. 2007: Magmatic evolution of the Peñón Rosado granite: Petrogenesis of garnet-bearing granitoids. *Lithos* 95, 177–207.
- Deer W.A., Howie R.A. & Zussman J. 1996: An introduction to the rock-forming minerals. John Wiley and Sons, New York, 1–528.
- Deer W.A., Howie R.A. & Zussman J. 2001: An introduction to the rock-forming minerals. Second Edition. Longman, London, 1–972.
- Dymek R.F. 1983: Titanium, aluminum and interlayer cation substitutions in biotite from high-grade gneisses West Greenland. *Amer. Mineralogist* 68, 880–889.
- Ewart A. & Stipp J.J. 1968: Petrogenesis of the volcanic rocks of the central North Island, New Zealand, as indicated by a study of $\text{Sr}^{87}/\text{Sr}^{86}$ ratios, and Sr, Rb, K, U and Th abundances. *Geochim. Cosmochim. Acta* 32, 699–736.
- Foster M.D. 1960: Interpretation of the composition of trioctahedral micas. *USGS Professional Paper* 354-B, 11–49.
- Frost B.R. & Frost C.D. 2008: A geochemical classification of feldspathic igneous rocks. *J. Petrology* 54, 1–15.
- Goswami S., Bhownik S.K. & Dasgupta S. 2009: Petrology of a non-classical Barrovian inverted metamorphic sequence from the western Arunachal Himalaya, India. *J. Asian Earth Sci.* 36, 390–406.
- Green T.H. 1978: A model for the formation and crystallization of corundum-normative calc-alkaline magmas through amphibole fractionation: a discussion. *J. Geol.* 86, 269–275.
- Guo Z. & Wilson M. 2012: The Himalayan leucogranites: Constraints on the nature of their crustal source region and geodynamic setting. *Gondwana Research* 22, 360–376.
- Harris N.B.W. & Inger S. 1992: Geochemical characteristics of pelite-derived granites. *Contr. Mineral. Petrology* 110, 46–56.
- Harris N.B.W., Pearce J.A. & Tindle A.G. 1986: Geochemical characteristics of collision-zone magmatism. In: Coward M.P. & Ries A.C. (Eds.): Collision tectonics. *Geol. Soc. London, Spec. Publ.* 19, 67–81.
- Harris N.B.W., Inger S. & Xu R.H. 1990: Cretaceous plutonism in central Tibet: An example of post-collision magmatism? *J. Volcanol. Geotherm. Res.* 44, 21–32.
- Harris N., Ayres M. & Massey J. 1995: The incongruent melting of muscovite: implications for the geochemistry and extraction of granite magmas. *J. Geophys. Res.* 100, 15777–15787.
- Harrison T.M., Grove M., Lovera O.M. & Catlos E.J. 1998: A model for the origin of Himalayan anatexis and inverted metamorphism. *J. Geophys. Res.* 103, 27017–27032.
- Heming R.F. & Carmichael I.S.E. 1973: High-temperature pumice flows from the Rabaul Caldera, Papua New Guinea. *Contr. Mineral. Petrology* 38, 1–20.
- Henry D.J., Guidotti C.V. & Thomson J.A. 2005: The Ti-saturation surface for low-to-medium pressure metapelitic biotite: Implications for the formation of metapelitic rocks. *J. Metamorph. Geology* 23, 1–18.

- cations for geothermometry and Ti- substitution mechanisms. *Amer. Mineralogist* 90, 316–328.
- Holtz F. & Johannes W. 1991: Genesis of peraluminous granites I. Experimental investigation of melt compositions at 3 and 5 kb and various H₂O activities. *J. Petrology* 32, 935–58.
- Inger S. & Harris N. 1993: Geochemical constraints on leucogranite magmatism in the Langthan Valley, Nepal Himalaya. *J. Petrology* 34, 345–368.
- Ishihara S. 1977: The magnetite-series and ilmenite-series granitic rocks. *Mining Geology* 27, 293–305.
- Jiang Y.H., Ling H.F., Jiang S.Y., Fan H.H., Shen W.Z. & Ni P. 2005: Petrogenesis of a Late Jurassic Peraluminous Volcanic complex and its high-Mg, potassic, quenched enclaves at Xiangshan, Southeast China. *J. Petrology* 46, 6, 1121–1154.
- Karimpour M.H., Stern C.R. & Mourad M. 2011: Chemical composition of biotite as a guide to petrogenesis of granitic rocks from Maherabad, Dehnow, Gheshlagh, Khajehmourad and Najmabad, Iran, Iranian. *J. Crystallography and Mineralogy* 18, 89–100.
- Lalonde A.E. & Bernard P. 1993: Composition and color of biotite from granites: two useful properties in the characterization of plutonic suites from the Hepburn internal zone of Wopmay orogen, Northwest Territories. *Canad. Mineralogist* 31, 203–217.
- Le Breton N. & Thompson A.B. 1988: Fluid-absent (dehydration) melting of biotite in metapelites in the early stages of crustal anatexis. *Contr. Mineral. Petrology* 99, 226–237.
- Le Fort P., Cuney M., Deniel C., France-Lanord C., Sheppard S.M.F., Upreti B.N. & Vidal P. 1987: Crustal generation of the Himalayan leucogranites. *Tectonophysics* 134, 39–57.
- Luth W.C., Jahns R.H. & Tuttle O.F. 1964: The granite system at pressures of 4 to 10 kilobars. *J. Geophys. Res.* 69, 759–773.
- Maniar P.D. & Piccoli P.M. 1989: Tectonic discrimination of granitoids. *Geol. Soc. Amer. Bull.* 101, 635–643.
- McDermott F., Harris N.B. & Hawkesworth C.J. 1996: Geochemical constraints on crustal anatexis: a case study from the Pan-African Damara granitoids of Namibia. *Contr. Mineral. Petrology* 123, 406–423.
- Miller C.F. 1985: Are strongly peraluminous magmas derived from pelitic sedimentary sources? *J. Geology* 93, 673–689.
- Miller C.F., Stoddard E.F., Bradfish L.J. & Dollase W.A. 1981: Composition of plutonic muscovite. Genetic implications. *Canad. Mineralogist* 19, 25–34.
- Mohajel M., Fergusson C.L. & Sahandi M.R. 2003: Cretaceous-Tertiary convergence and continental collision, Sanandaj-Sirjan zone, Western Iran. *J. Asian Earth Sci.* 21, 397–412.
- Nabelek P.I., Russ-Nabelek C. & Denison J.R. 1992: The generation and crystallization conditions of the Proterozoic Harney Peak leucogranite, Black Hills, South Dakota, USA: Petrologic and geochemical constraints. *Contr. Mineral. Petrology* 110, 173–191.
- Nachit H. 1986: Contribution à l'étude analytique et expérimentale des biotites des granitoïdes. Applications typologiques. *Tese de Doutorado, Université de Bretagne Occidentale*, Brest, 1–238.
- Patiño-Douce A.E. 1999: What do experiments tell us about the relative contributions of crust and mantle to the origins of granitic magmas? In: Castro A., Fernandez C. & Vigneresse J.L. (Eds.): Understanding granites. Integrating new and classical techniques. *Geol. Soc. London, Spec. Publ.* 158, 55–75.
- Patiño-Douce A.E. & Beard J.A. 1995: Dehydration-melting of biotite gneiss and quartz amphibolite from 3 to 15 kbar. *J. Petrology* 36, 707–738.
- Patiño-Douce A.E. & Harris N. 1998: Experimental constraints on Himalayan anatexis. *J. Petrology* 39, 689–710.
- Patiño-Douce A.E. & Johnston A. 1991: Phase equilibria and melt productivity in the pelitic system: implications for the origin of peraluminous granitoids and aluminous granulites. *Contr. Mineral. Petrology* 107, 202–218.
- Paul A., Hatzfeld D., Kaviani A., Tatar M. & Pequegnat C. 2010: Seismic imaging of the lithospheric structure of the Zagros mountain belt (Iran). *Geol. Soc. London, Spec. Publ.* 330, 5–18.
- Pearce J.A., Harris N.B.W. & Tindle A.G. 1984: Trace element discrimination diagrams for the tectonic interpretation of granitic rocks. *J. Petrology* 25, 956–983.
- Rollinson H. 1993: Using geochemical data: evaluation, presentation, and interpretation. *John Wiley*, New York, 1–352.
- Sahandi M.A., Radfar J., Hosseini Doust J. & Mohajel M. 2007: Geological map of Shazand, Scale 1: 100,000. *Geological Survey of Iran*.
- Sawyer E.W. 1996: Melt segregation and magma flow in migmatites: implications for the generation of granite magmas. *Trans. Roy. Soc. Edinburgh Earth Sci.* 87, 85–94.
- Scaillet B., France-Lanord C. & Le Fort P. 1990: Badrinath-Gangotri plutons (Garhwal, India): petrological and geochemical evidence for fractionation processes in high Himalayan leucogranite. *J. Volcanol. Geotherm. Res.* 44, 163–88.
- Searle M.P., Cottle J.M., Streule M.J. & Waters D.J. 2010: Crustal melt granites and migmatites along the Himalaya: melt source, segregation, transport and granite emplacement mechanisms. *Trans. Roy. Soc. Edinburgh. Earth Sci.* 100, 219–233.
- Sepahi A.A., Shahbazi H., Siebel W. & Ranin A. 2014: Geochronology of plutonic rocks from the Sanandaj-Sirjan zone, Iran and new zircon and titanite U-Th-Pb ages for granitoids from the Marivan pluton. *Geochronometria* 41, 207–215.
- Shabani A.A.T., Lalonde A.E. & Whalen J.B. 2003: Composition of biotite from granitic rocks of the Canadian Appalachian orogen: A potential tectonomagmatic indicator? *Canad. Mineralogist* 41, 1381–1396.
- Soesoo A. 2000: Fractional crystallization of mantle derived melts as a mechanism for some I-type granite petrogenesis: an example from Lachlan Fold Belt, Australia. *J. Geol. Soc. London* 157, 135–149.
- Speer J.A. 1984: Micas in igneous rocks. In: Bailey S.W. (Ed.): *Micas. Rev. Mineralogy* 13, 299–356.
- Stevens G., Clemens J.D. & Droop G.T.R. 1997: Migmatites, granites and granulites: The data from experiments on “primitive” metasedimentary protoliths. *Contr. Mineral. Petrology* 128, 352–370.
- Stevens G., Villaros A. & Moyen J.F. 2007: Selective peritectic garnet entrainment as the origin of geochemical diversity in S-type granites. *Geology* 35, 9–12.
- Sun S.S. & McDonough W.F. 1989: Chemical and isotopic systematics of oceanic basalts; implications for mantle composition and processes. In: Saunders A.D. & Norry M.J. (Eds.): Magmatism in the ocean basins. *Geol. Soc. London, Spec. Publ.* 42, 313–345.
- Sylvester P.J. 1998: Post-collisional strongly peraluminous granites. *Lithos* 45, 29–44.
- Takin M. 1972: Iranian geology and continental drift in the Middle East. *Nature* 235, 147–150.
- Taylor J., Stevens G., Armstrong R. & Kisters A.F.M. 2010: Granulite facies anatexis in the Ancient Gneiss Complex, Swaziland, at 2.73 Ga: mid crustal metamorphic evidence for mantle heating of the Kaapvaal craton during Venterdorp magmatism. *Precambrian Res.* 177, 88–102.
- Thompson A.B. 1982: Dehydration melting of pelitic rocks and the generation of H₂O undersaturated granitic liquids. *Amer. J. Sci.* 282, 1567–1595.
- Villaros A., Stevens G. & Buick I.S. 2009: Tracking S-type granite from source to emplacement: clues from garnet in the Cape Granite Suite. *Lithos* 112, 217–235.
- Villaseca C., Orejana D., Paterson B.A., Billstrom K. & Perez-Soba C. 2007: Metaluminous pyroxene-bearing granulite xenoliths

- from the lower continental crust in central Spain: their role in the genesis of Hercynian I-type granites. *Eur. J. Mineral.* 19, 463–477.
- Waters D.J. 2001: The significance of prograde and retrograde quartz-bearing intergrowth microstructures in partially melted granulite-facies rocks. *Lithos* 56, 97–110.
- Watson E.B. & Harrison T.M. 1983: Zircon saturation revisited: temperature and composition effects in a variety of crustal magma types. *Earth Planet. Sci. Lett.* 64, 295–304.
- Watt G.R. & Harley S.L. 1993: Accessory phase controls on the geochemistry of crustal melts and restites produced during water undersaturated partial melting. *Contr. Mineral. Petrology* 114, 550–566.
- White A.J.R. & Chappell B.W. 1988: Some supracrustal (S-type) granites of the Lachlan Fold Belt. *Trans. Roy. Soc. Edinburgh Earth Sci.* 79, 169–181.
- Whitney J.A. 1988: The origin of granite: the role and source of water in the evolution of granitic magmas. *Geol. Soc. Amer. Bull.* 100, 1886–1897.
- Whitney D.L. & Evans B.W. 2010: Abbreviations for name of rock-forming minerals. *Amer. Mineralogist* 95, 185–187.
- Williamson B.J., Shaw A., Downes H. & Thirlwall M.F. 1996: Geochemical constraints on the genesis of Hercynian two-mica leucogranites from the Massif Central, France. *Chem. Geol.* 127, 25–42.
- Wones D.R. 1989: Significance of the assemblage titanite + magnetite + quartz in granitic rocks. *Amer. Mineralogist* 74, 744–749.
- Wones D.R. & Eugster H.P. 1965: Stability of biotite: experiment, theory, and application. *Amer. Mineralogist* 50, 1228–1272.
- Zane A. & Rizzo G. 1999: The compositional space of muscovite in granitic rocks. *Canad. Mineralogist* 37, 1229–1238.
- Zen E. 1988: Phase relations of peraluminous granitic rocks and their petrogenetic implications. *Ann. Rev. Earth Planet. Sci.* 16, 21–51.